Interaction between β-Purothionin and Dimyristoylphosphatidylglycerol: A ^{31}P-NMR and Infrared Spectroscopic Study

Julie-Andrée Richard,* Isabelle Kelly,* Didier Marion,† Michel Pézolet,* and Michèle Auger*
*Département de Chimie, Centre de Recherche en Sciences et Ingénierie des Macromolécules, Université Laval, Québec G1K 7P4, Canada; and †Institut National de la Recherche Agronomique, Laboratoire de Biochimie et Technologie des Protéines, 44316 Nantes Cedex 03, France

ABSTRACT The interaction of β-purothionin, a small basic and antimicrobial protein from the endosperm of wheat seeds, with multilamellar vesicles of dimyristoylphosphatidylglycerol (DMPG) was investigated by ^{31}P solid-state NMR and infrared spectroscopy. NMR was used to study the organization and dynamics of DMPG in the absence and presence of β-purothionin. The results indicate that β-purothionin does not induce the formation of nonlamellar phases in DMPG. Two-dimensional exchange spectroscopy shows that β-purothionin decreases the lateral diffusion of DMPG in the fluid phase. Infrared spectroscopy was used to investigate the perturbations, induced by β-purothionin, of the polar and nonpolar regions of the phospholipid bilayers. At low concentration of β-purothionin, the temperature of the gel-to-fluid phase transition of DMPG increases from 24°C to ~33°C, in agreement with the formation of electrostatic interactions between the cationic protein and the anionic phospholipid. At higher protein concentration, the lipid transition is slightly shifted toward lower temperature and a second transition is observed below 20°C, suggesting an insertion of the protein in the hydrophobic core of the lipid bilayer. The results also suggest that the presence of β-purothionin significantly modifies the lipid packing at the surface of the bilayer to increase the accessibility of water molecules in the interfacial region. Finally, orientation measurements indicate that the α-helices and the β-sheet of β-purothionin have tilt angles of ~60° and 30°, respectively, relative to the normal of the ATR crystal.

INTRODUCTION

Plants contain molecules that allow their protection against pathogenic agents such as fungi and bacteria. Among these molecules are purothionins, which are small basic globular proteins found in the endosperm of wheat seeds (*Triticum aestivum*) (Balls et al., 1942). Three genetic variants exist, namely α_1-, α_2-, and β-purothionin (Fernandez de Caleya et al., 1976), all ~5 kDa and containing 45 amino acid residues. Due to the presence of several basic amino acid residues, purothionins are positively charged at neutral pH. The three-dimensional (3D) structure of purothionins has been solved by NMR spectroscopy (Clore et al., 1986, 1987) and by x-ray diffraction (Rao et al., 1995; Stec et al., 1995) and can be represented by the Greek capital letter gamma (Γ). The vertical arm consists of two antiparallel α-helices and the horizontal arm contains a coil in extended conformation and a short antiparallel β-sheet. This tertiary structure is stabilized by salt bridges, intramolecular hydrogen bonds, and four disulfide bridges. Purothionins have an amphipathic character with the hydrophobic residues located at the outer surface of the two α-helices, and the hydrophilic residues situated at the inner surface of the Γ and at the outer surface of the corner of the Γ (Clore et al., 1986; Teeter et al., 1981).

An important property of purothionins is their toxicity toward many living organisms such as bacteria, yeast, and fungi (Stuart and Harris, 1942; Fernandez de Caleya et al., 1972), animals (Coulson et al., 1942), cultured mammalian cells (Nakanishi et al., 1979; Carrasco et al., 1981) and insect larvae (Kramer et al., 1979). Other biological activities have been observed in vitro (for a review see Bohlmann and Apel, 1991; Florack and Stiekema, 1994), but the main biological function of purothionins appears to be related to the defense of plants against their microbial predators. Most of the observed biological activities result from the interaction of purothionins with the target cell membrane (Carrasco et al., 1981). This is strengthened by the fact that several thionins interact with phospholipid bilayers and natural membranes (Caaveiro et al., 1997, 1998; Huang et al., 1997; Hughes et al., 2000; Thevissen et al., 1996).

Huang et al. (1997) have studied the interaction between *Pyrularia* thionin, an analog of purothionins, and large unilamellar vesicles (LUV) of dipalmitoylphosphatidylglycerol (DPPG) by differential scanning calorimetry (DSC). The results obtained indicated that at low concentration of protein, the gel-to-fluid phase transition temperature of DPPG increases, in agreement with the formation of electrostatic interactions between the thionin and the lipid vesicles. However, at higher concentrations of protein, a decrease of the phase transition temperature and the appearance of a second transition at a lower temperature were observed. As the thionin concentration increased, only the low-temperature phase transition was detected. This low-temperature transition has been associated with the insertion in the hydrophobic core of the DPPG bilayer of the

Submitted February 4, 2002, and accepted for publication May 15, 2002.
Address reprint requests to Michèle Auger, Département de Chimie, CERSIM, Université Laval, Québec G1K7P4, Canada. Tel.: 418-656-3393; Fax: 418-656-7916; E-mail: michele.auger@chm.ulaval.ca.

0006-3495/02/10/2074/10 $2.00

tryptophan residue located in the hydrophobic part of the α-helices. This study suggested that the interaction between the thionin and the lipid could involve a two-step mechanism. First, the protein adsorbs to the bilayer surface through electrostatic interactions, and second, penetrates the hydrophobic bilayer region through a mechanism driven by the thionin tryptophan.

Caaveiro et al. (1997) have investigated the interaction between α-purothionin and large unilamellar vesicles composed of phosphatidylcholine (PC), phosphatidylglycerol (PG), and the mixture PC/PG (1:1). Their results indicate that α-purothionin induces the aggregation of the negatively charged vesicles and causes the release of the fluorescent probes encapsulated in the vesicles. In addition, these effects depend on the lipid composition and only occur when the vesicles contain negatively charged phospholipids. From this study, Caaveiro et al. have concluded that the protein induces membrane leakage that causes the release of the intracellular material. They have also studied the effect of the insertion of distearoylphosphatidylethanolamine-polyethylene glycol 2000 (PEG-PE) in the bilayer on the aggregation and permeability of the vesicles (Caaveiro et al., 1998). Their results indicate that PEG-PE prevents the aggregation of the vesicles while it does not prevent the binding of purothionin to the vesicles and, therefore, the release of fluorescent probes. Hence, the presence of PEG-PE at the surface of the membrane separates two processes that otherwise would be taking place simultaneously, i.e., membrane permeabilization and aggregation.

More recently, it has been shown that ion channels are formed in model lipid membranes composed of PE/PC 2:1 and PS/PE/PC 2:2:1 upon addition of α_1-, α_2-, or β-purothionin (Hughes et al., 2000). However, other results have shown that fluorescent probes are released from vesicles in the presence of α-purothionin even though these probes are too large to go through the ion channels formed by the protein. This implies that the bilayer must necessarily be destructured to allow the release of large molecules (Caaveiro et al., 1998), in agreement with the fact that the α-helices of purothionins are too short to span a lipid bilayer (Caaveiro et al., 1998).

To better understand the mode of action of purothionins, we have investigated the interaction between β-purothionin and multilamellar vesicles (MLV) of dimyristoylphosphatidylglycerol, a negatively charged phospholipid, using both ^{31}P solid-state NMR and Fourier transform infrared spectroscopy.

Solid-state ^{31}P-NMR spectroscopy is a valuable technique to study the different phases formed by model phospholipid membranes. The spectra of the different lipid phases (e.g., gel and fluid lamellar phases, inverted hexagonal phase, and isotropic phases such as small vesicles and micelles) are characterized by a specific lineshape (Seelig, 1978; Smith and Ekiel, 1984). Also, ^{31}P-NMR allows the study of the dynamics of the lipid headgroup. In the present study we have investigated the lateral diffusion of the phospholipids in the plane of the membrane using two-dimensional (2D) exchange spectroscopy (Fenske and Jarrell, 1991). This technique uses the fact that in solid-state NMR, the chemical shielding shows an orientational dependence in the static magnetic field. Therefore, it is possible to observe correlation peaks in a 2D spectrum map representing an orientational exchange originating from the diffusion of the lipids over the curved membrane surface. In this study, NMR spectroscopy has been used to determine how β-purothionin affects the organization of DMPG membranes and the lateral diffusion of the phospholipids.

Fourier transform infrared spectroscopy (FTIR) is well-suited for the study of lipid-protein interactions because it allows the investigation of the conformation of phospholipid molecules at different levels in the lipid bilayers and to follow structural changes that occur during the gel-to-fluid phase transition. Moreover, it can provide information on the secondary structure of proteins in lipid bilayers. Therefore, we have used FTIR to study how β-purothionin affects the acyl chains, the interfacial region, and the phosphate groups of DMPG bilayers. Furthermore, with the use of polarized infrared radiation, it has been possible to determine the orientation of the protein relative to the bilayer.

MATERIALS AND METHODS

Materials

Dimyristoylphosphatidylglycerol was purchased from Avanti Polar Lipids (Alabaster, AL) and used without further purification. Purothionins were extracted from wheat seeds using a modification of the procedures previously described for the purification of puroindolines (Blochet et al., 1993; Dubreil et al., 1997). Briefly, 4 kg of wheat endosperm flour were extracted with 10 l of Tris 100 mM, pH 7.8, NaCl 0.1 M, EDTA 5 mM containing 5% Triton X-114. After stirring for 12 h at 4°C and centrifugation at 8,000 × *g* for 30 min, the supernatant was heated at 30°C to allow phase partitioning. The upper detergent-poor phase was discarded. The lower detergent-rich phase was recovered, diluted five times with water, and loaded on a column packed with a cation exchanger (SP Biobeads, Pharmacia, U.K.). As highlighted by SDS PAGE, purothionins eluted as a single peak just after puroindolines and the corresponding collected fractions were pooled and dyalized against deionized water. After freeze-drying, purothionins were separated in α_1, α_2, and β-purothionin by semi-preparative reversed-phase HPLC on a column packed with Nucleosil C18 5 μ 300 Å with a gradient from 0.1% TFA in deionized water to 0.1% TFA in CH_3CN. The corresponding fractions were collected and freeze-dried after dilution with deionized water. The purity of the purified fractions was controlled by mass spectrometry as previously described (Douliez et al., 2001).

Sample preparation

NMR experiments

Pure DMPG dispersions (20% w/v) were prepared by adding an aqueous solution containing 20 mM NaCl and 1 mM EDTA to the solid lipids. The pH of the lipid dispersion was measured with a microelectrode (Microelectrodes, Londonderry, NH) and adjusted to 7.0 with diluted NaOH or HCl. To obtain a homogenous dispersion, the sample was heated at ~40°C for 5 min, stirred on a vortex mixer, and cooled in liquid nitrogen. This

cycle was repeated at least five times to obtain multilamellar vesicles. The lipid/protein complexes were prepared by mixing the lipid dispersion (20 mg DMPG) and a protein solution made in 20 mM NaCl and 1 mM EDTA. The protein concentration was adjusted to yield the desired lipid-to-protein molar ratios and the pH was verified and adjusted to 7.0 if necessary. The lipid-protein mixtures were then heated (40°C), stirred, and cooled (10°) at least five times.

FTIR experiments

The lipid dispersion (10%, w/v) and protein solution (2%, w/v) were prepared in 150 mM NaCl made in H_2O or D_2O. Deuterated water was used to eliminate the spectral interference due to the bending vibration mode of water in the 1600–1700 cm^{-1} region. The pH of these samples was measured and adjusted to 7.0 with diluted NaOH and HCl (or NaOD and DCl). To obtain a homogenous DMPG dispersion, freeze-thawing was applied as described above. The DMPG/β-purothionin complexes were prepared by mixing the appropriate volumes of lipid dispersion and protein solution to obtain lipid-to-protein molar ratios of 30:1, 15:1, and 10:1. The pH of the lipid-protein mixtures was verified and adjusted to 7.0 if necessary. The complexes were formed by five heating-cooling cycles as described above.

NMR measurements

The ^{31}P-NMR spectra were acquired at 121.5 MHz on a Bruker ASX-300 spectrometer (Bruker Canada Ltd., Milton, ON) operating at a ^{1}H frequency of 300.0 MHz. Experiments were carried out with a broadband/^{1}H dual-frequency 4-mm probehead. One-dimensional spectra (2200 scans for DMPG and 7000 scans for the complexes) were recorded using a Hahn echo pulse sequence under conditions of proton decoupling during the acquisition (Rance and Byrd, 1983). The 90° pulse length was ~4.5 μs, the interpulse delay τ was 30 μs, and the recycle time was 4 s. A line-broadening of 200 Hz was applied to all spectra.

Two-dimensional spectra were acquired using the NOESY pulse sequence with TPPI to give quadrature detection in both dimensions (Bodenhausen et al., 1984):

$$90^\circ_x - t_1 - 90^\circ_x - t_m - 90^\circ_x - t_2 \qquad (1)$$

where t_1 is the evolution time, t_m is the mixing time, and t_2 is the detection period. The t_m were varied from 50 μs to 200 ms, the 90° pulse length was ~4.5 μs, and the recycle time was 4 s. The data sets contained 512 points in the $F2$ dimensions and 64 points in the $F1$ dimension, zero-filled to 512 to obtain a square matrix. Ninety-six scans were recorded for each serial file in given 2D experiments. A line-broadening of 200 Hz was applied to all spectra in the $F2$ dimension. For all 1D and 2D experiments, the spectral width was 50 kHz and the chemical shifts (expressed in ppm) were referenced relative to the signal of phosphoric acid at 0 ppm.

To determine the correlation time for lateral diffusion, the method described by Picard et al. (1998) was used. This method is based on the calculation of the time-dependent orientational autocorrelation function of order 2, $C_2(t_m)$:

$$C_2(t_m) = \frac{5}{\delta^2}\frac{\iint \omega_1\omega_2 S(\omega_1, \omega_2; t_m)\mathrm{d}\omega_1 d\omega_2}{\iint S(\omega_1, \omega_2; t_m)\mathrm{d}\omega_1 d\omega_2} \qquad (2)$$

where t_m is the mixing time, δ is the chemical shift, and ω_1 and ω_2 are the frequencies before and after the mixing time. Because both δ and ω are expressed in frequency units, the C_2 values are dimensionless. The autocorrelation function, $C_2(t_m)$, decays exponentially with the mixing time and the decay factor is the correlation time for the lateral diffusion, t_d:

$$C_2(t_m) = \exp\left(-\frac{t_m}{t_d}\right) \qquad (3)$$

FTIR measurements

The infrared spectra were recorded on a Nicolet Magna 550 (Thermo-Nicolet, Madison, WI) Fourier transform infrared spectrometer equipped with a narrow-band mercury-cadmium-telluride detector and a germanium-coated KBr beam-splitter. For the recording of transmission spectra, ~12 μl of sample was inserted between two BaF_2 windows separated by a 6-μm Mylar spacer in a homemade cell thermoelectrically regulated (Pézolet et al., 1983). A total of 200 scans were averaged at a resolution of 2 cm^{-1} and a spectrum was recorded every 2°C between 0 and 50°C. For polarized attenuated total internal reflectance (ATR) measurements, an ATR unit (Harrick Scientific Co., Ossining, NY) and a parallelogram germanium ATR crystal (50 × 20 × 2 mm, 45°) were used. Before use, the crystal was first cleaned with chloroform and then in a plasma cleaner sterilizer (Harrick Scientific Co.). Oriented films were prepared by spreading ~30 μl of the aqueous sample on the germanium ATR crystal. The sample was then dried and the crystal was placed in the ATR unit. For each polarization (parallel (p) and perpendicular (s) to the plane of incidence), a total of 250 scans were averaged at room temperature.

All spectral manipulations were performed with the Grams 386 software (Galactic Industries Corporation, Salem, NH). The spectra in the CH_2 region (3030–2770 cm^{-1}) were baseline-corrected using a cubic function. In the carbonyl and phosphate regions (1680–1780 cm^{-1} and 995–1320 cm^{-1}, respectively), the baseline correction was done with a quadratic function. The spectra in the amide bands region (1380–1720 cm^{-1}) were baseline-corrected using a linear function in the case of β-purothionin and a quadratic function in the case of the DMPG/β-purothionin complexes. The position of the band due to the CH_2 symmetric C–H stretching mode was determined by calculating the center of gravity of the bands at 85% of their height (Cameron et al., 1982) and the carbonyl bands were deconvolved according to the method of Kauppinen et al. (1981).

To determine the orientation of the α-helices and β-sheet of β-purothionin and of the DMPG acyl chains, the dichroic ratios $R^{ATR} = (A_p/A_s)$ were calculated from the height of the bands. For the DMPG acyl chains, this height was measured at 2850 cm^{-1} and for the α-helices, at 1664 cm^{-1}. For the β-sheet, the height was measured at 1635 and 1530 cm^{-1} in the region of the amide I band and amide II band, respectively.

For a system with both axial symmetry (e.g., acyl chains, α-helices) and uniaxial orientation, an order parameter $\langle P_2(\cos\theta)\rangle$ with respect to the normal to the ATR crystal can be determined with the following equation (Fringeli and Günthard, 1981):

$$\langle P_2(\cos\theta)\rangle = \left\langle\frac{3\cos^2\theta - 1}{2}\right\rangle = \frac{E_x^2 - R^{ATR}E_y^2 + E_z^2}{E_x^2 - R^{ATR}E_y^2 + E_z^2}\cdot\frac{2}{3\cos^2\gamma - 1} \qquad (4)$$

where R^{ATR} is the dichroic ratio, γ is the angle between the transition moment of a given vibration and the chain axis, and E_x^2, E_y^2, and E_z^2 are the mean-squared electric fields along the x, y, and z directions, respectively. Values of 1.954, 2.303, and 2.651 along the x, y, and z directions, respectively, were calculated for the mean-squared electric fields using the Harrick thick film approximation (Harrick, 1967) with refractive indices of 1.45 and 4.00 for the film and the germanium crystal, respectively, and an angle of incidence of 45°. Angles γ of 90° and 38° have been used for the acyl chains in the all-*trans* conformation and the α-helices, respectively (Buffeteau et al., 2000; Marsh et al., 2000). Assuming an infinitely narrow

distribution of orientation (Lafrance et al., 1995; Johansson and Lindblom, 1980), an angle θ can be determined from the order parameter $\langle P_2(\cos\theta)\rangle$. A value of 1 for the order parameter $\langle P_2(\cos\theta)\rangle$ is obtained for perfect orientation along the reference direction ($\theta = 0°$), while a value of -0.5 is obtained for perfect perpendicular orientation ($\theta = 90°$). Unordered structures or structures perfectly oriented at 54.7° will yield a value of the order parameter of 0.

Equation 4 cannot be used to calculate the orientation of a nonaxially symmetric system such as a β-sheet. To define the orientation of a β-sheet, two dichroic ratios are required. Marsh (1997) has developed equations to determine the orientation of β-sheets using the dichroic ratio of both the amide I and amide II bands (Eqs. 5 and 6). This method assumes that the resultant transition moment of a β-sheet is oriented parallel ($\Theta = 0°$) to the β-strand axis for the amide II vibration and perpendicular ($\Theta = 90°$) to this axis for the amide I vibration. A combination of the dichroic ratios obtained for both the amide I and amide II bands allows a complete definition of the orientation of the β-sheet.

$$R^{\mathrm{ATR}}(\Theta = 0°) = \frac{E_x^2}{E_y^2} + \frac{2\langle\cos^2\theta\rangle\langle\cos^2\alpha\rangle}{1 - \langle\cos^2\theta\rangle\langle\cos^2\alpha\rangle}\cdot\frac{E_z^2}{E_y^2} \quad (5)$$

$$R^{\mathrm{ATR}}(\Theta = 90°) = \frac{E_x^2}{E_y^2} + \frac{2\langle\cos^2\theta\rangle\langle\sin^2\alpha\rangle}{1 - \langle\cos^2\theta\rangle\langle\sin^2\alpha\rangle}\cdot\frac{E_z^2}{E_y^2} \quad (6)$$

In these equations, Θ is the angle between the transition moment and the chains axis, and E_x^2, E_y^2, and E_z^2 are the mean-squared electric fields along the x, y, and z directions, respectively. Equations 5 and 6 allow calculation of the tilt angle, θ, of a β-sheet relative to the normal to the crystal and the tilt angle, α, of the chains inside the β-sheet. It is considered that the angle α is the same for all the β-strands constituting a β-sheet.

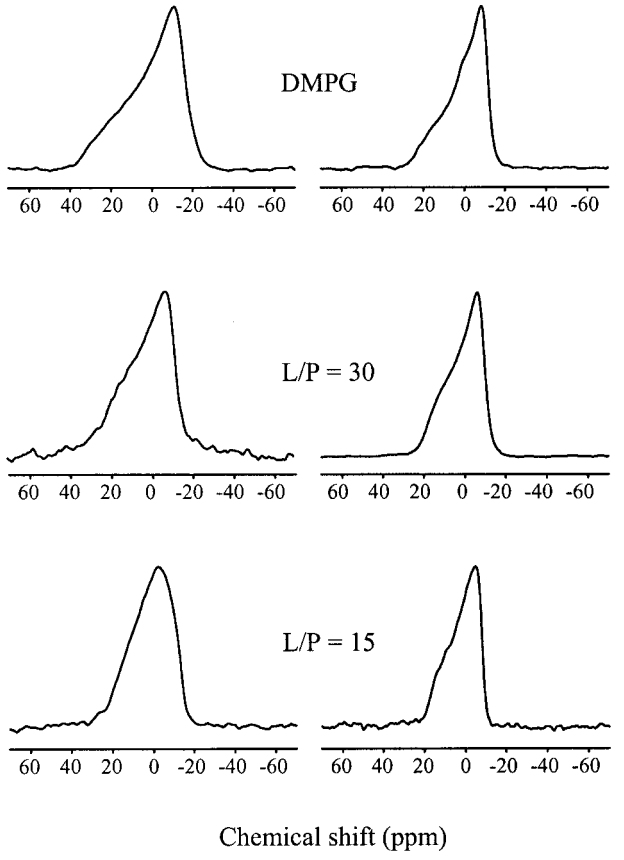

FIGURE 1 ^{31}P-NMR spectra obtained at 10°C (*left*) and 40°C (*right*) for pure DMPG and for DMPG/β-purothionin complexes at lipid-to-protein molar ratios of 30:1 and 15:1.

RESULTS AND DISCUSSION

^{31}P-NMR results

Spectral lineshapes

The phase behavior of aqueous dispersions of DMPG in the absence and presence of β-purothionin has first been investigated. The ^{31}P-NMR spectra of pure DMPG and of DMPG/β-purothionin complexes at 10 and 40°C are shown in Fig. 1. As expected, the results show that the spectral width decreases with increasing temperature as the lipid undergoes the transition from the gel phase to the fluid phase. The smaller spectral width obtained in the fluid phase can be explained by an increased disordering of the lipid headgroup (Smith and Ekiel, 1984). In addition, the spectra obtained for both the pure DMPG and the DMPG/β-purothionin complexes at lipid-to-protein molar ratios of 30:1 and 15:1 are characteristic of a lamellar phase (Seelig, 1978). This indicates that the presence of β-purothionin does not induce the formation of nonbilayer phases. Even though it has been suggested that the protein disrupts the lipid bilayer (Carrasco et al., 1981; Huang et al., 1997), the results obtained here do not show any evidence of the formation of small isotropic vesicles (Picard et al., 1996). However, the widths of the spectra obtained for the complex at a lipid-to-protein molar ratio of 15:1 are slightly smaller than those observed for the pure lipid, indicating that the presence of a large proportion of protein could induce an increased disordering of the lipid headgroup.

The DMPG/β-purothionin complex at a lipid-to-protein molar ratio of 10:1 has also been investigated, but it has been impossible in this case to obtain an NMR spectrum with an acceptable signal-to-noise ratio. When the protein solution was added to the lipid dispersion, the complex precipitated. This could be due to the aggregation of the multilayered vesicles, resulting in a much broader NMR signal.

The results presented in Fig. 1 also indicate that the addition of the protein causes a shift of the NMR spectra toward higher chemical shift values in both the gel and fluid phases. This can be explained by the nature of the interaction between β-purothionin and DMPG. More specifically, the presence of a positive charge near the negatively charged phosphate groups decreases the electronic density around the phosphorus nucleus, and consequently the spectrum is shifted toward higher chemical shift values (Akitt, 1992). This behavior shows that electrostatic interactions occur when β-purothionin binds to DMPG.

Lateral diffusion

^{31}P two-dimensional solid-state NMR spectroscopy (Fenske and Jarrell, 1991) has been used to determine how β-purothionin affects the slow motions ($<10^3$ Hz) of the lipids and more specifically, the lateral diffusion of DMPG. In two-dimensional ^{31}P-EXSY solid-state NMR spectra, cross-intensity appears when there is a change of orientation during the mixing time t_m and results in a square spectrum. In the case of spherical vesicles, two main motions contribute to the change in the orientation of the phospholipids: the tumbling, characterized by the correlation time t_t, and the lateral diffusion, characterized by the correlation time t_d (Fenske and Jarrell, 1991). The correlation time measured experimentally, t_e, is related to the correlation time due to the diffusion, t_d, and the correlation time due to tumbling, t_t (Eq. 7):

$$\frac{1}{t_e} = \frac{1}{t_t} + \frac{1}{t_d} \tag{7}$$

where

$$t_t = \frac{4\pi\eta r^3}{3kT} \tag{8}$$

and

$$t_d = \frac{r^2}{6D_t} \tag{9}$$

In these equations, η is the viscosity of the solvent, k is the Boltzmann constant, r is the radius of the vesicles, T is the temperature, and D_t is the diffusion constant.

In the fluid phase, the change in orientation is mainly due to the lateral diffusion of the lipids. Indeed, since the mean calculated radius for vesicles prepared by dispersion varies between 1.0 and 1.2 μm (Fenske and Jarrell, 1991), the correlation time due to tumbling is ~0.8–1.4 s (Eq. 8). The t_d values for the lateral diffusion being of the order of a millisecond, $1/t_d \gg 1/t_t$ and thus, $t_e = t_d$. Therefore, tumbling can be neglected.

The lateral diffusion of pure DMPG and of DMPG/β-purothionin complexes at lipid-to-protein molar ratios of 30:1 and 15:1 has been investigated. Fig. 2 shows the 2D spectra obtained with mixing times of 50 μs and 5 ms for pure DMPG and the two complexes. At short mixing time (Fig. 2, *left*), the intensity is mainly located on the diagonal, indicating that there is little or no lateral diffusion. At a longer mixing time (Fig. 2, *right*), the off-diagonal spectral intensity becomes more important, which indicates that the lipids change their orientation during the mixing time and, therefore, that lateral diffusion occurs. If we compare the spectra obtained for the complexes (Fig. 2, *middle* and *bottom*) with those of pure DMPG (Fig. 2, *top*), little difference is seen. However, the calculation of the autocorrelation time functions C_2 as a function of mixing time (Fig. 3) clearly indicates differences between the systems studied and allows determination of the correlation time for the lateral diffusion, t_d. The correlation time obtained for the pure DMPG system is 4 ms and correlation times of 8 and 17 ms have been obtained for the complexes at lipid-to-protein molar ratios of 30:1 and 15:1, respectively. These results indicate that β-purothionin decreases the lateral diffusion of the DMPG and therefore, that the protein could act as an obstacle to the lipid diffusion.

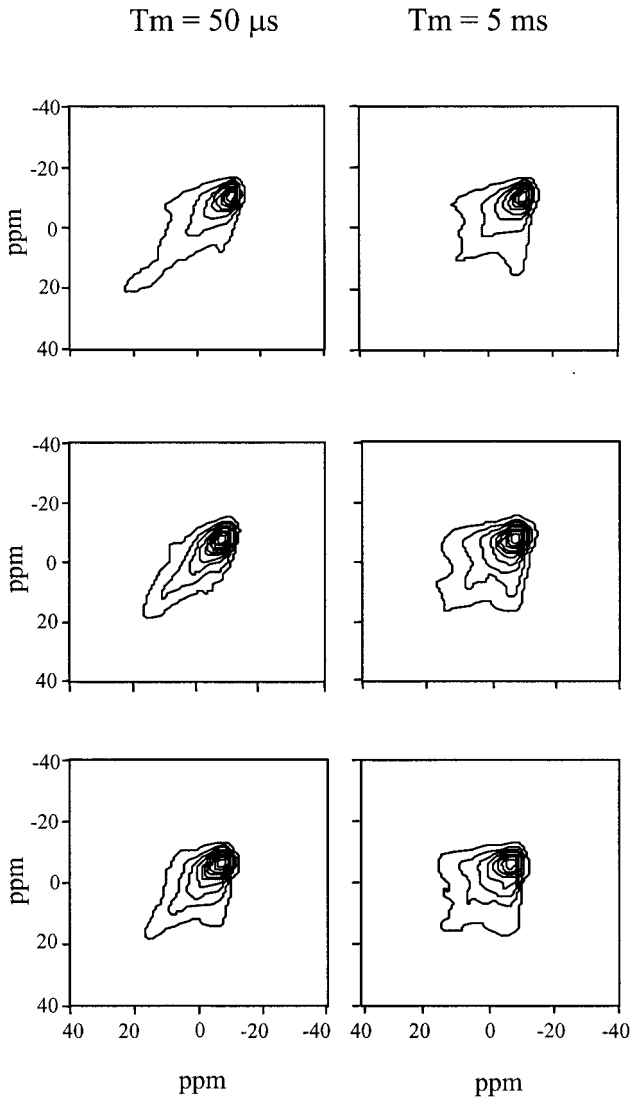

FIGURE 2 2D ^{31}P-NMR spectra of pure DMPG (*top*) and of DMPG/β-purothionin complexes at lipid-to-protein molar ratios of 30:1 (*middle*) and 15:1 (*bottom*) at 40°C for mixing times of 50 μs and 5 ms.

Infrared spectroscopy results

Lipid membrane structure

To determine how β-purothionin interacts with DMPG, we have investigated the effects of the protein on the acyl

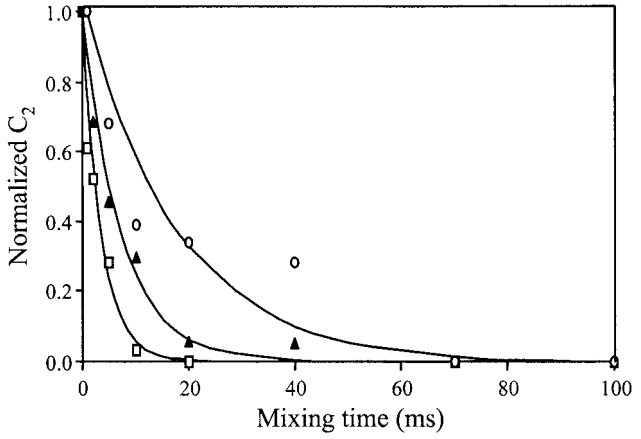

FIGURE 3 Normalized C_2 as a function of mixing time for pure DMPG (□) and for DMPG/β-purothionin complexes at lipid-to-protein molar ratios of 30:1 (▲) and 15:1 (○).

chains, the interfacial region (C=O), and the polar headgroup (PO_2^-) of DMPG bilayers by infrared spectroscopy.

To evaluate the effect of β-purothionin on the lipid acyl chains, we have investigated the symmetric CH_2 stretching mode (2850 cm^{-1}) because it is almost unaffected by underlying contributions from the protein component (Surewicz et al., 1987). The evolution of the frequency of the symmetric methylene stretching mode of the pure DMPG acyl chains as a function of temperature shows a discontinuity at the gel-to-fluid transition temperature (T_m) (Fig. 4), due to the important increase in the proportion of *gauche* conformers at T_m (Mendelsohn and Mantsch, 1986; Lewis and McElhaney, 1998). From these results, a phase transition temperature of 25°C is obtained for pure DMPG, in agreement with the value of 24°C found in the literature (Marsh, 1990). The addition of β-purothionin at a lipid-to-protein molar ratio of 30:1 shifts the phase transition temperature to 32°C. For the lipid-to-protein molar ratio of 15:1, the main phase transition is observed near 31°C, but a second transition is observed at 18°C. For the complex at a lipid-to-protein molar ratio of 10:1, the high-temperature phase transition occurs near 30°C and the low-temperature transition is further shifted to 16°C (Fig. 4).

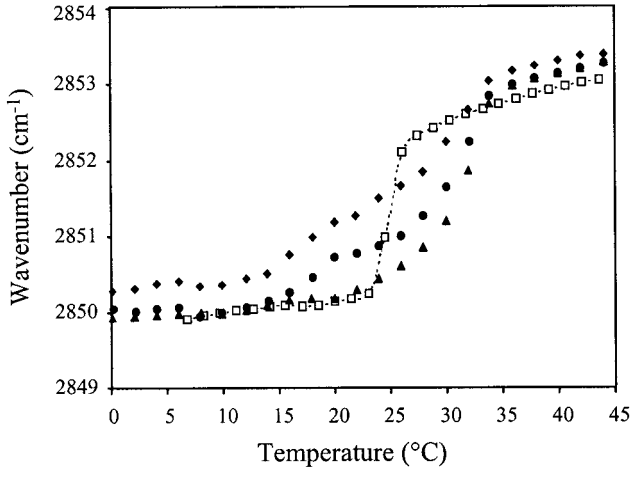

FIGURE 4 Temperature dependence of the CH_2 symmetric stretching vibration of pure DMPG (□) and of DMPG/β-purothionin complexes at lipid-to-protein molar ratios of 30:1 (▲), 15:1 (●), and 10:1 (◆).

An increase of the phase transition temperature of phospholipids is generally observed in the case of electrostatic interactions with proteins and polypeptides (Paphadjopoulos et al., 1975; Carrier et al., 1997). More specifically, it has been shown that an increase of T_m is associated with the stabilization of the charges between the protein and the lipid, leading to an increase of the order of the acyl chains and to the stabilization of the gel phase in the presence of protein (Surewicz and Epand, 1986). The results presented in Fig. 4 also indicate that the acyl chains are perturbed by the presence of the protein. Indeed, for the complex at a lipid-to-protein molar ratio of 10:1 in the gel phase and for all the complexes in the fluid phase, the wavenumbers of the methylene stretching band are higher in the lipid-protein systems than those observed for the pure DMPG bilayers. This observation shows that the presence of β-purothionin results in a decrease of the conformational order of the lipid acyl chains, suggesting the insertion of the protein in the lipid bilayer in addition to the electrostatic interaction discussed above.

The presence of a second phase transition at lower temperature for the complexes with lipid-to-protein molar ratios of 15:1 and 10:1 also supports the existence of hydrophobic interactions between the protein and the membrane. Indeed, by inserting into the bilayer, the hydrophobic residues of the protein would cause a decrease of the acyl chain order. Thus, the phospholipids in direct contact with the protein would have a phase transition temperature lower than that of the lipids that do not interact directly with the protein. This thermotropic behavior is similar to that observed by Huang et al. (1997) in a DSC study on the interaction of the thionin of *Pyrularia pubera* and dipalmitoylphosphatidylglycerol (DPPG) vesicles. In this study, the decrease of the high-temperature phase transition and the appearance of a low-temperature phase transition have been associated with the insertion in the hydrophobic core of the lipid bilayer of the tryptophan residue, located in the hydrophobic part of the α-helices. Our results suggest that the binding of β-purothionin to DMPG membranes is similar to that of the *Pyrularia pubera* thionin to DPPG. However, a tyrosine residue also located in the hydrophobic part of the α-helices would insert in the bilayer instead of a tryptophan. The strong electrostatic and hydrophobic interactions between β-purothionin and DMPG suggested by the infrared results are in agreement with the decrease of the lipid lateral diffusion observed by 2D ^{31}P-NMR spectroscopy.

The interfacial region of the phospholipid bilayers has also been investigated using the carbonyl stretching vibra-

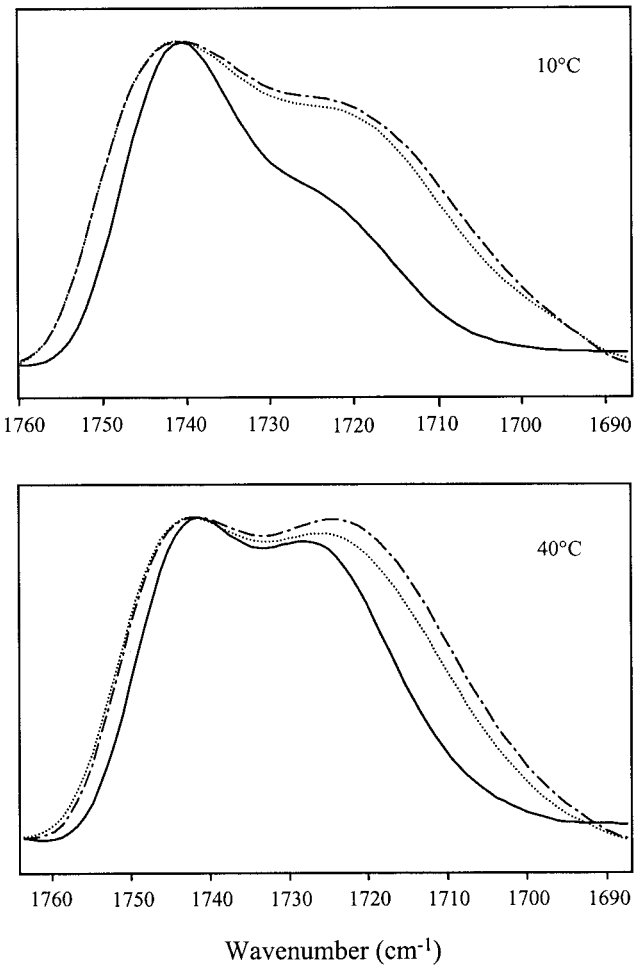

FIGURE 5 Infrared spectra in the lipid carbonyl stretching mode region for pure DMPG (*solid line*) and for DMPG/β-purothionin complexes at lipid-to-protein molar ratios of 30:1 (*dotted line*) and 15:1 (*dot-dashed line*).

tion between 1700 and 1750 cm^{-1} (Casal and Mantsch, 1984). Only one band is generally observed in this spectral region for hydrated samples, but the Fourier deconvolution technique (Kauppinen et al., 1981) allows enhancing the resolution and revealing two overlapping bands. The band at 1725 cm^{-1} is associated with carbonyl groups involved in hydrogen bonds, while the band at 1740 cm^{-1} is associated with free carbonyl groups (Blume et al., 1988). The intensity ratio of these two bands is therefore useful for monitoring the hydration of the interfacial region of a lipid bilayer.

Fig. 5 shows the deconvolved spectra in the carbonyl region at 10 and 40°C for DMPG in D_2O in the absence and in the presence of β-purothionin. For pure DMPG, the relative intensity of the hydrogen-bonded carbonyl component (1725 cm^{-1}) increases when the lipids undergo the gel-to-fluid phase transition. This behavior can be explained by the fact that the hydrocarbon chains become more disordered at high temperature, facilitating the penetration of water in the interfacial region of the bilayer. The proportion of C=O groups bonded to water molecules is therefore more important in the fluid phase. The results presented in Fig. 5 also indicate that the bonded C=O band is shifted from 1723 cm^{-1} to 1728 cm^{-1} from the gel to the fluid phase. This can be explained by the fact that at high temperature, the hydrogen bond between the lipid C=O group and the deuterium atoms of the solvent are weaker than at low temperature and, consequently, this band is shifted toward higher wavenumbers (Carrier et al., 1997).

For the lipid/protein complexes, the results indicate that the relative intensity of the hydrogen-bonded carbonyl component increases compared to that of pure DMPG and this, in both the gel and fluid phases. Two hypotheses can be suggested. On one hand, β-purothionin could favor the penetration of water in the interfacial region or, on the other hand, hydrogen bonds could be formed between the carbonyl groups of DMPG and the amino acid side chains of β-purothionin. It has been shown that the increase of the relative intensity of the hydrogen-bonded carbonyl component is generally associated with the formation of hydrogen bonds between C=O groups and protons (or deuterium atoms) of the solvent (Désormeaux et al., 1992; Carrier et al., 1997; Arrondo and Goni, 1998; Nabet et al., 1994). Therefore, our results are consistent with the hypothesis that β-purothionin would modify the DMPG bilayer sufficiently to increase the accessibility of the water molecules in the interfacial region, as also suggested by Huang et al. (1997). However, the existence of hydrogen bonds between the lipid carbonyl groups and the β-purothionin amino acid side chains cannot be ruled out from our results.

The study of the phosphate group absorption bands between 900 and 1300 cm^{-1} (Fringeli and Günthard, 1981) allows characterizing the polar headgroups of phospholipids (Arrondo and Goni, 1998). More specifically, a perturbation of the phosphate bands suggests the presence of an interaction between a protein and the membrane surface. The results obtained in the present study (not shown) indicate that the phosphate bands of DMPG are not significantly perturbed by the presence of β-purothionin. This behavior is in agreement with that observed in the study of the interaction between DMPG and other basic proteins (Surewicz et al., 1987).

Orientation measurements

The orientation of the α-helices and the β-sheet of β-purothionin for lipid/protein complexes at lipid-to-protein molar ratios of 30:1, 15:1, and 10:1 and the orientation of the lipid acyl chains in pure DMPG and in all the complexes has also been investigated. Fig. 6 shows the polarized ATR spectra of the DMPG/β-purothionin complex (30:1) in the CH and amide I and II regions. In addition, Table 1 presents the dichroic ratios, the order parameters, and the tilt angles of

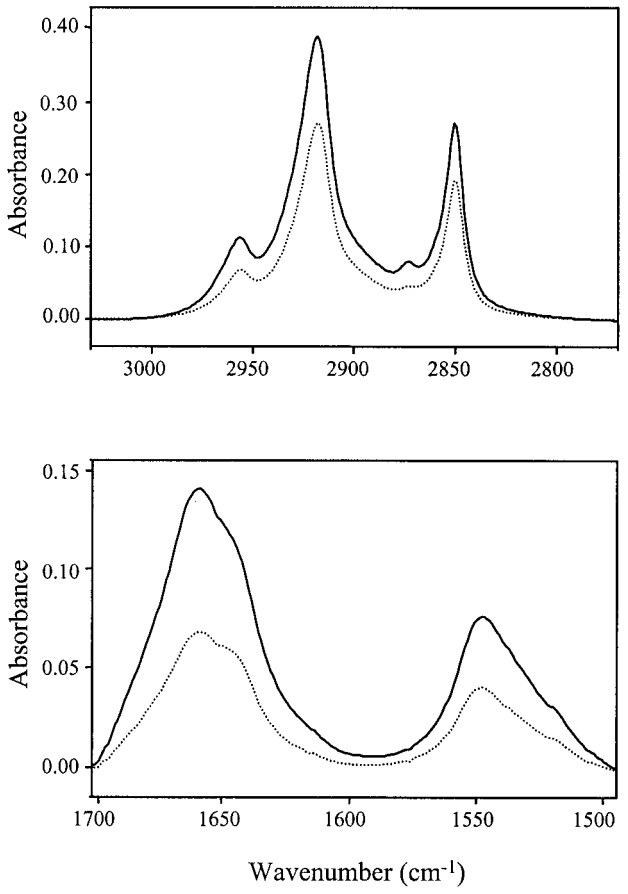

FIGURE 6 S (*dotted line*) and p-polarized (*solid line*) ATR spectra in the C–H stretching region (*top*) and in the amide I and amide II spectral region (*bottom*) obtained in the fluid phase (40°C) for the DMPG/β-purothionin complex at a lipid-to-protein molar ratio of 30:1.

the α-helices, β-sheet, and lipid acyl chains. These values are the average of three independent measurements. The tilt angles θ have been calculated assuming an infinitely narrow distribution of orientation (Lafrance et al., 1995; Johansson and Lindblom, 1980).

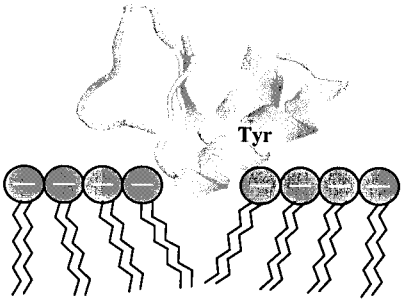

FIGURE 7 Model of interaction between β-purothionin and the negatively charged DMPG membrane.

The results presented in Table 1 indicate that the α-helices have an order parameter $\langle P_2(\cos\theta)\rangle$ between −0.08 and −0.16 as a function of the lipid-to-protein molar ratios, corresponding to tilt angles between 58° and 61° relative to the crystal normal. Within experimental errors, these tilt angles do not vary significantly as a function of the lipid-to-protein molar ratio. However, an order parameter $\langle P_2(\cos\theta)\rangle$ of 0.63 was obtained for the β-sheet, corresponding to a tilt angle of 30°. Although the angle obtained for the α-helices is close to 54.7°, the angle of an isotropic distribution, the combination of tilt angles obtained for both the α-helices and the β-sheet, is consistent with an orientation of β-purothionin relative to the DMPG membrane as illustrated in Fig. 7.

The acyl chains of pure DMPG have an order parameter $\langle P_2(\cos\theta)\rangle$ of 0.72, corresponding to an orientation of 26° relative to the crystal normal, assuming an infinitely narrow distribution of orientation. This is in close agreement with the angle of 29° obtained by x-ray diffraction (Pascher et al., 1987). When β-purothionin is added at lipid-to-protein molar ratios of 30:1, 15:1, and 10:1, the order parameter $\langle P_2(\cos\theta)\rangle$ considerably decreases from 0.72 for pure DMPG to values between 0.48 and 0.58 in the complexes, indicating an increased conformational disorder of the lipid acyl chains. This behavior is in agreement with the partial insertion of the protein in the bilayer, as suggested above.

TABLE 1 Orientation of the α-helices, the β-sheet, and the lipid acyl chains in DMPG/β-purothinin complexes as a function of the lipid-to-protein molar ratio

Molar Ratio (L/P)	α-Helices			β-Sheet			Acyl Chains		
	R^{ATR}	$\langle P_2(\cos\theta)\rangle$	θ	R^{ATR}	$\langle P_2(\cos\theta)\rangle$	θ	R^{ATR}	$\langle P_2(\cos\theta)\rangle$	θ
∞	—	—	—	—	—	—	1.08	0.72	26°
30:1	1.89	−0.08	58°	1.74 (I) 1.65 (II)	0.63	30°	1.32	0.48	36°
15:1	1.78	−0.16	61°	1.72 (I) 1.64 (II)	0.63	30°	1.25	0.56	33°
10:1	1.78	−0.16	61°	1.71 (I) 1.62 (II)	0.63	30°	1.22	0.58	32°

R^{ATR}, dichroic ratio; $\langle P_2(\cos\theta)\rangle$, order parameter; θ, tilt angle. (I) refers to the dichroic ratio in the amide I region and (II) to the dichroic ratio in the amide II region.

Within experimental error, no significant differences are observed between the different lipid-to-protein molar ratios.

CONCLUSIONS

The interaction between DMPG bilayers and β-purothionin has been investigated in the present study by ^{31}P-NMR and infrared spectroscopy. The ^{31}P-NMR results indicate that the organization of the lipid bilayer is not significantly affected by the presence of β-purothionin and that the protein decreases the lateral diffusion of DMPG. However, the results obtained by infrared spectroscopy demonstrate the existence of an electrostatic interaction between DMPG and β-purothionin and a partial insertion of the protein in the lipid membrane. Orientation measurements are consistent with a model in which the α-helices and the β-sheet have tilt angles of ~60° and 30°, respectively, relative to the DMPG membrane.

This work was supported by the Natural Science and Engineering Research Council (NSERC) of Canada, by the Fonds pour la Formation de Chercheurs et pour l'Aide à la Recherche (FCAR) from the province of Québec, and by the Centre de Recherche en Sciences et Ingénierie des Macromolécules (CERSIM). J.-A.R. also thanks NSERC for the award of a postgraduate scholarship.

REFERENCES

Akitt, J. W. 1992. NMR and Chemistry. An Introduction to Modern NMR Spectroscopy. Chapman and Hall, London.

Arrondo, J. L. R., and F. M. Goni. 1998. Infrared studies of protein-induced perturbation of lipids in lipoproteins and membranes. *Chem. Phys. Lipids.* 96:53–68.

Balls, A. K., W. S. Hale, and T. H. Harris. 1942. A crystalline protein obtained from a lipoprotein of wheat flour. *Cereal Chem.* 19:279–288.

Blochet, J.-E., C. Chevalier, E. Forest, E. Pebay-Peroula, M.-F. Gautier, P. Joudrier, M. Pézolet, and D. Marion. 1993. Complete amino acid sequence of puroindoline, a new basic and cystine-rich protein with a unique tryptophan-rich domain, isolated from wheat endosperm by Triton X-114 phase partitioning. *FEBS Lett.* 329:336–340.

Blume, A., W. Hübner, and G. Messner. 1988. Fourier transform infrared spectroscopy of ^{13}C=O labeled phospholipids hydrogen bonding to carbonyl groups. *Biochemistry.* 27:8239–8249.

Bodenhausen, G., H. Kogler, and R. R. Ernst. 1984. Selection of coherence-transfer pathways in NMR pulse experiments. *J. Magn. Reson.* 58:370–388.

Bohlmann, H., and K. Apel. 1991. Thionins. *Annu. Rev. Plant Physiol. Plant Mol. Biol.* 42:227–240.

Caaveiro, J. M. M., A. Molina, J. M. Gonzalez-Manas, P. Rodriguez-Palenzuela, F. Garcia-Olmedo, and F. M. Goni. 1997. Differential effects of five types of antipathogenic plant peptides on model membranes. *FEBS Lett.* 410:338–342.

Caaveiro, J. M. M., A. Molina, P. Rodriguez-Palenzuela, F. M. Goni, and J. M. Gonzalez-Manas. 1998. Interaction of wheat α-thionin with large unilamellar vesicles. *Protein Sci.* 7:2567–2577.

Cameron, D. G., J. K. Kauppinen, D. J. Moffatt, and H. H. Mantsch. 1982. Precision in condensed phase vibrational spectroscopy. *Appl. Spectros.* 36:245–250.

Carrasco, L., D. Vazquez, C. Hernandez-Lucas, P. Carbonero, and F. Garcia-Olmedo. 1981. Thionins: plant peptides that modify membrane permeability in cultured mammalian cells. *Eur. J. Biochem.* 116: 185–189.

Carrier, D., N. Chartrand, and W. Matar. 1997. Comparison of the effects of amikacin and kanamycins A and B on dimyristoylphosphatidylglycerol bilayers. An infrared spectroscopic investigation. *Biochem. Pharmacol.* 53:401–408.

Casal, H. L., and H. H. Mantsch. 1984. Polymorphic phase behavior of phospholipid membranes studied by infrared spectroscopy. *Biochim. Biophys. Acta.* 779:381–401.

Clore, G. M., M. Nilges, D. K. Sukumaran, A. T. Brünger, M. Karplus, and A. M. Gronenborn. 1986. The three-dimensional structure of α1-purothionin in solution: combined use of nuclear magnetic resonance, distance geometry and restrained molecular dynamics. *EMBO J.* 5:2729–2735.

Clore, G. M., D. K. Sukumaran, A. M. Gronenborn, M. M. Teeter, M. Whitlow, and B. L. Jones. 1987. Nuclear magnetic resonance study of the solution structure of α1-purothionin. *J. Mol. Biol.* 193:571–578.

Coulson, E. J., T. H. Harris, and B. Axelrod. 1942. Effect on small laboratory animals of the injection of the crystalline hydrochloride of a sulfur protein from wheat flour. *Cereal Chem.* 19:301–307.

Désormeaux, A., G. Laroche, P. E. Bougis, and M. Pézolet. 1992. Characterization by infrared spectroscopy of the interaction of a cardiotoxin with phosphatidic acid and binary mixtures of phosphatidic acid and phosphatidylcholine. *Biochemistry.* 31:2173–2182.

Douliez, J.-P., C. Pato, H. Rabesona, D. Molle, and D. Marion. 2001. Disulfide bond assignment, lipid transfer activity and secondary structure of a 7-kDa plant lipid transfer protein, LPT2. *Eur. J. Biochem.* 268:1400–1403.

Dubreil, L., J. P. Compoint, and D. Marion. 1997. Interactions of puroindolines with wheat flour polar lipids determine their foaming properties. *J. Agric. Food Chem.* 45:108–116.

Fenske, D. B., and H. C. Jarrell. 1991. Phosphorus-31 two-dimensional solid-state exchange NMR. *Biophys. J.* 59:55–69.

Fernandez de Caleya, R., B. Gonzalez-Pascual, F. Garcia-Olmedo, and P. Carbonero. 1972. Susceptibility of phytopathogenic bacteria to wheat purothionins in vitro. *Appl. Microbiol.* 23:998–1000.

Fernandez de Caleya, R., C. Hernandez-Lucas, P. Carbonero, and F. Garcia-Olmedo. 1976. Gene expression in alloploids: genetic control of lipopurothionins in wheat. *Genetics.* 83:687–699.

Florack, D. E. A., and W. J. Stiekema. 1994. Thionins: properties, possible biological roles and mechanisms of action. *Plant Mol. Biol.* 26:25–37.

Fringeli, U. P., and H. H. Günthard. 1981. Infrared membrane spectroscopy. *In* Membrane Spectroscopy. E. Grell, editor. Springer-Verlag, Berlin. 270–332.

Harrick, N. J. 1967. Internal Reflection Spectroscopy. Harrick Scientific Corp., Ossining, NY.

Huang, W., L. P. Vernon, L. D. Hansen, and J. D. Bell. 1997. Interactions of thionin from *Pyrularia pubera* with dipalmitoylphosphatidylglycerol large unilamellar vesicles. *Biochemistry.* 36:2860–2866.

Hughes, P., E. Dennis, M. Whitecross, D. Llewellyn, and P. Gage. 2000. The cytotoxic plant protein, β-purothionin, forms ion channels in lipid membranes. *J. Biol. Chem.* 275:823–827.

Johansson, L. B.-Å, and G. Lindblom. 1980. Orientation and mobility of molecules in membranes studied by polarized light spectroscopy. *Q. Rev. Biophys.* 13:63–118.

Kauppinen, J. K., D. J. Moffatt, and H. H. Mantsch. 1981. Fourier self-deconvolution: a method for resolving intrinsically overlapped bands. *Appl. Spectrosc.* 35:271–276.

Kramer, K. J., L. W. Klassen, B. L. Jones, R. D. Speirs, and A. E. Kammer. 1979. Toxicity of purothionin and its homologues of the tobacco hornworm, *Manduca sexta* (L.) (Lepidoptera: Sphingidae). *Toxicol. Appl. Pharmacol.* 48:179–183.

Lafrance, C. P., A. Nabet, R. E. Prud'homme, and M. Pézolet. 1995. On the relationship between the order parameter $\langle P_2(\cos\theta)\rangle$ and the shape of the orientation distributions. *Can. J. Chem.* 73:1497–1505.

Lewis, R. N. A. H., and R. N. McElhaney. 1998. The structure and organization of phospholipid bilayers as revealed by infrared spectroscopy. *Chem. Phys. Lipids.* 96:9–21.

Marsh, D. 1990. Handbook of Lipid Bilayers. CRC Press, Inc., Boston.

Marsh, D. 1997. Dichroic ratios in polarized Fourier transform infrared for nonaxial symmetry of β-sheet structures. *Biophys. J.* 72:2710–2718.

Mendelsohn, R., and H. H. Mantsch. 1986. Fourier transform infrared studies of lipid-protein interaction. *In* Progress in Protein-Lipid Interactions. W. D. Pont, editor. Elsevier, New York. 103–146.

Nabet, A., J. M. Boggs, and M. Pézolet. 1994. Study by infrared spectroscopy of the interaction of bovine myelin basic protein with phosphatidic acid. *Biochemistry.* 33:14792–14799.

Nakanishi, T., H. Yoshizumi, S. Tahara, A. Hakura, and K. Toyoshima. 1979. Cytotoxicity of purothionin-A on various animal cells. *Jpn. J. Cancer Res. (Gann).* 70:323–326.

Paphadjopoulos, D., M. Moscarello, E. H. Eylan, and T. Isac. 1975. Effects of proteins on thermotropic phase transitions of phospholipid membranes. *Biochim. Biophys. Acta.* 401:317–335.

Pascher, I., S. Sundell, K. Harlos, and H. Eibl. 1987. Conformation and packing properties of membrane lipids: the crystal structure of sodium dimyristoylphosphatidylglycerol. *Biochim. Biophys. Acta.* 896:77–88.

Pézolet, M., B. Boulé, and D. Bourque. 1983. Thermoelectrically regulated sample holder for Raman spectroscopy. *Rev. Sci. Instrum.* 54: 1364–1367.

Picard, F., M.-J. Paquet, E. J. Dufourc, and M. Auger. 1998. Measurement of the lateral diffusion of dipalmitoylphosphatidylcholine adsorbed on silica beads in the absence and presence of melittin: a ^{31}P two-dimensional exchange solid-state NMR study. *Biophys. J.* 74:857–868.

Picard, F., M. Pézolet, P. E. Bougis, and M. Auger. 1996. Model of interaction between a cardiotoxin and dimyristoylphosphatidic acid bilayers determined by solid-state ^{31}P-NMR spectroscopy. *Biophys. J.* 70:1737–1744.

Rance, M., and R. A. Byrd. 1983. Obtaining high-fidelity spin ½ powder spectra in anisotropic media: phase-cycled Hahn echo spectroscopy. *J. Magn. Reson.* 52:221–240.

Rao, U., B. Stec, and M. M. Teeter. 1995. Refinement of purothionins reveals solute particles important for lattice formation and toxicity. 1. α1-Purothionin revisited. *Acta Crystallogr.* D51:904–913.

Seelig, J. 1978. ^{31}P nuclear magnetic resonance and the head group structure of phospholipids in membranes. *Biochim. Biophys. Acta.* 515: 105–140.

Smith, I. C. P., and I. H. Ekiel. 1984. Phosphorus-31 NMR of phospholipids in membranes. *In* Phosphorus-31 NMR. Principles and Applications. D. Gorenstein, editor. Academic Press, London. 447–475.

Stec, B., U. Rao, and M. M. Teeter. 1995. Refinement of purothionins reveals solute particles important for lattice formation and toxicity. 2. Structure of β-purothionin at 1.7 Å resolution. *Acta Crystallogr.* D51: 914–924.

Stuart, L. S., and T. H. Harris. 1942. Bactericidal and fungicidal properties of a crystalline protein isolated from unbleached wheat flour. *Cereal Chem.* 19:288–300.

Surewicz, W. K., and R. M. Epand. 1986. Phospholipid structure determines the effects of peptides on membranes. Differential scanning calorimetry studies with pentagastrin-related peptides. *Biochim. Biophys. Acta.* 856:290–300.

Surewicz, W. K., M. A. Moscarello, and H. H. Mantsch. 1987. Fourier transform infrared spectroscopic investigation of the interaction between myelin basic protein and dimyristoylphosphatidylglycerol bilayers. *Biochemistry.* 26:3881–3886.

Teeter, M. M., J. A. Mazer, and J. L'Italien. 1981. Primary structure of the hydrophobic plant protein crambin. *Biochemistry.* 20:5437–5443.

Thevissen, K., A. Ghazi, G. W. De Samblanx, C. Brownlee, R. W. Osborsn, and W. F. Broekaert. 1996. Fungal membrane responses induced by plant defensins and thionins. *J. Biol. Chem.* 271:15018–15025.